Available online at www.sciencedirect.com
ScienceDirect
Bioorganic & Medicinal Chemistry 16 (2008) 5021–5029
Bioorganic & Medicinal Chemistry

Interaction between artemisinin and heme. A Density Functional Theory study of structures and interaction energies

Jocley Queiroz Araújo,[a] José Walkimar de Mesquita Carneiro,[a,b,*] Martha Teixeira de Araujo,[c] Franco Henrique Andrade Leite[d,e] and Alex Gutterres Taranto[d,e]

[a]*Programa de Pós-Graduação em Química Orgânica, Universidade Federal Fluminense, Outeiro de São João Batista, s/n, 24020-150, Niterói, RJ, Brazil*
[b]*Departamento de Química Inorgânica, Universidade Federal Fluminense, Outeiro de São João Batista, s/n, 24020-150, Niterói, RJ, Brazil*
[c]*Departamento de Físico-Química, Universidade Federal Fluminense, Outeiro de São João Batista, s/n, 24020-150, Niterói, RJ, Brazil*
[d]*Programa de Pós-Graduação em Biotecnologia, Universidade Estadual de Feira de Santana, Br 116, km 03, 44031-460, Feira de Santana, BA, Brazil*
[e]*Departamento de Saúde, Universidade Estadual de Feira de Santana, Br 116, km 03, 44031-460, Feira de Santana, BA, Brazil*

Received 22 August 2007; revised 11 March 2008; accepted 13 March 2008
Available online 16 March 2008

Abstract—Malaria is an infectious disease caused by the unicellular parasite *Plasmodium* sp. Currently, the malaria parasite is becoming resistant to the traditional pharmacological alternatives, which are ineffective. Artemisinin is the most recent advance in the chemotherapy of malaria. Since it has been proven that artemisinin may act on intracellular heme, we have undertaken a systematic study of several interactions and arrangements between artemisinin and heme. Density Functional Theory calculations were employed to calculate interaction energies, electronic states, and geometrical arrangements for the complex between the heme group and artemisinin. The results show that the interaction between the heme group and artemisinin at long distances occurs through a complex where the iron atom of the heme group retains its electronic features, leading to a quintet state as the most stable one. However, for interaction at short distances, due to artemisinin reduction by the heme group, the most stable complex has a septet spin state. These results suggest that a thermodynamically favorable interaction between artemisinin and heme may happen.

1. Introduction

Malaria is a non-contagious disease of chronic evolution that manifests in acute episodes.[1] It has been described as the most prevalent and severe infection among the tropic diseases, resurging again in several countries where it was eliminated or greatly reduced.[2] Currently, millions of people in the tropical and subtropical zones of the world are afflicted by malaria.[3]

The most prevalent type of malaria is caused by the unicellular parasite *Plasmodium* sp., which may be injected in the blood stream when bitten by the female of the *Anopheles* mosquito.[1–3] Recently, the parasite has acquired resistance to the traditional clinical treatments, which are now ineffective.[2] The best advance in the chemotherapy of malaria in the last few years comes from the natural product artemisinin. Artemisinin (Fig. 1) was isolated from *Artemisia annua* L., a herb with antimalarial activity described more than five hundred years

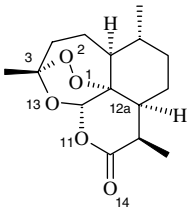

Figure 1. Artemisinin plan molecular representation with number indication of selected atoms.

Keywords: Artemisinin; Heme; DFT; Intermolecular interaction; Malaria.
* Corresponding author. Tel.: +55 21 26292174; fax: +55 21 26292129; e-mail: walk@vm.uff.br

0968-0896/$ - see front matter © 2008 Elsevier Ltd. All rights reserved.
doi:10.1016/j.bmc.2008.03.033

ago.[4,5] Studies have shown that administration of artemisinin to patients with malaria results in clinical improvement, followed by parasite elimination from the blood stream in two days.[6] Chemically, artemisinin is a sesquiterpene lactone having an endoperoxide bridge, which appears to be essential for its antimalarial activity,[5] since derivatives lacking the endoperoxide function, for example, deoxoartemisinin, are inactive.[5,7]

Studies suggested that the antimalarial activity of artemisinin is due to the interaction of its peroxide group with the prosthetic heme group of human hemoglobin.[8] Reduction of the peroxide group may lead to cytotoxic free radicals and electrophilic intermediates, which may be able to react with specific malaria membrane-associated proteins, leading to the parasite's death.[8] Moreover, artemisinin could inhibit hemoglobin degradation, heme polymerization, and interact with hemozoin, resulting in the split of the malarial pigment.[9] Experiments suggested that artemisinin can interrupt the process of heme detoxification by transferring an O-atom to heme, creating an iron–oxene derivative.[10] On the other hand, it has also been found that the trioxane unit of artemisinin can act as a source of hydroperoxide, providing electrophilic oxygenating species, hydroxyl or alkoxyl radicals, via reductive cleavage of the peroxide bond by the iron ion of heme. Thus, these species would be able to hydroxylate biomolecules or to abstract hydrogen atoms, leading to the parasite's death.[11,12] In conclusion, these results have been rationalized as giving evidence that artemisinin degradation starts with one electron transfer from the heme Fe^{2+} ion to the peroxide bond, leading to the formation of radical anions that promote subsequent reactions.[13–16] These conclusions have been further supported by experiments in an aqueous environment which propose that the reaction of artemisinin with the iron ion originates products with antimalarial activity.[17]

The previous studies therefore strongly suggest that the heme group is the most probable target for artemisinin action. Thus, the heme–artemisinin interaction constitutes the initial stage of the mechanism of action of artemisinin. Determination of the energies and relative orientations of both unities upon interaction may contribute to increase knowledge on the mechanism of action of artemisinin. With this goal, we simulated the interaction between the heme group and the artemisinin molecule by means of Density Functional Theory calculations. We determined the interaction energies, electronic states of the heme–artemisinin complex and the geometrical arrangement for the thermodynamically most stable complex between the heme group and artemisinin.

2. Computational methods

The geometries of both artemisinin and the heme group were fully optimized using the Becke's three-parameter hybrid functional,[18] along with the non-local correlation functional of Lee, Yang, and Parr (B3LYP).[19,20] For the closed-shell artemisinin molecule the restricted formalism (B3LYP) was employed. For the heme group and the heme–artemisinin complex, with the d^6 Fe^{2+} ion (or d^5 Fe^{3+}), calculations were made with the unrestricted formalism (UB3LYP). In order to better represent the coordination environment found in hemoglobin, a histidine residue was added to one of the pseudoaxial positions of the heme unity (Fig. 2). This histidine unity is, as usual, coordinated to the iron Fe^{2+} ion through its sp^2 nitrogen atom. This will also allow for the Fe^{2+} ion to attain a nearly octahedral hexacoordinated arrangement after binding to the artemisinin molecule.

In order to be able to compare the results of these simple systems with those of the heme–artemisinin complex, two combinations of basis sets were used, which were denoted as hybrid basis set 1 and hybrid basis set 2. In the hybrid basis set 1, a combination of the STO-3G and the 3-21G basis set for the lighter elements and the LANL2DZ pseudopotential[21] for the iron atom was employed. The bigger basis set (3-21G) was defined for those atoms that might be directly involved in the reactions leading to the reduction of artemisinin and its further degradation (O_1, O_2, C_3, C_4, O_{11}, O_{13}, and $H_{4\alpha}$, see Fig. 1 for atom number), as well as the nitrogen atoms that are directly coordinated to the Fe^{2+} ion of the heme group. The remaining atoms were defined with the STO-3G basis set. In the hybrid basis set 2 we just replaced the STO-3G and the 3-21G basis set of the previous combination with the 3-21G and the 6-31G(d) basis set, respectively, for the corresponding atoms. The LANL2DZ was again employed for the Fe^{2+} ion. In order to compare results for a more representative basis set the structures of the heme group and of the artemisinin molecule were again fully optimized with the more robust 6-31G(d) basis set (LANL2DZ for Fe^{2+}). We refer to the last calculations as single basis set.

After calculating the isolated heme group and the artemisinin molecule we turned to the complex between them. The main goal of our approach was to study the arrangements that occur when the peroxide bond of artemisinin is as close as possible to the Fe^{2+} ion of heme. We did both, full geometry unrestricted optimizations and restricted optimizations, where the $Fe–O_2$ dis-

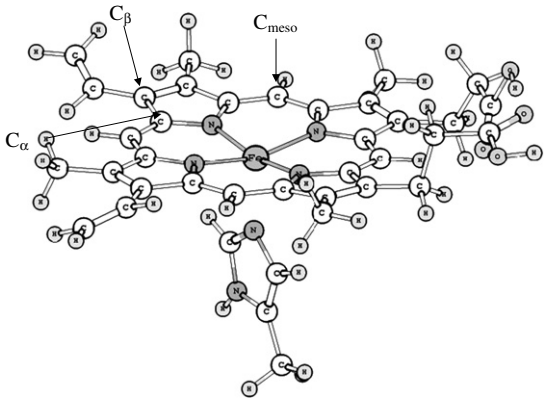

Figure 2. Heme prosthetic group coordinated to a histidine residue.

tance was taken as a kind of reaction coordinate. Thus, the heme–artemisinin complex was partially optimized for fixed Fe–O_2 distances of 2.0, 2.25, 2.5, 2.75, and 3.0 Å. The Fe–O_2 distance was chosen as the reaction coordinate because it has been shown that in the next step, after artemisinin reduction, a 1,5-hydride transfer from carbon C_4 to oxygen O_1 is the most probable pathway.[16] Therefore, the heme–artemisinin interaction should preferentially involve oxygen O_2 instead of O_1.

For both heme and the heme–artemisinin complex the calculations were done for at least three different spin controlled electronic states. The states with singlet, triplet and quintet multiplicities ($S = 0$, 1 and 2, respectively) were calculated for heme, while triplet, quintet, and septet states ($S = 1$, 2, and 3, respectively) were calculated for the complex between heme and artemisinin. For the unrestricted calculations the results were checked for spin contamination.

All calculations were done using the Gaussian03W package of molecular orbital calculation.[22]

3. Results and discussion

3.1. DFT calculations of artemisinin

The geometries of artemisinin and of the heme group were optimized with the combination of two basis sets indicated above and with the 6-31G(d) basis set. The objective was to check the performance of each basis set combination to reproduce experimental data, especially geometrical parameters. Additionally, atomic charges and spin densities obtained with the hybrid basis sets 1 and 2 were compared to those obtained with the 6-31G(d) basis set.

3.1.1. Atomic charges. Artemisinin atomic charges were calculated with two methodologies, the traditional Mulliken method and the Merz and Kollman method (MK).[23] The results for selected atoms are given in Table 1. As can be seen, the hybrid basis set 1 shows the most negative values of Mulliken charges concentrated on O_1, O_2, and O_{14}, while for MK charges the most negative values are on O_2, O_{13}, and O_{14} (Table 1 and Fig. 1). In both methods the oxygen atoms O_2 (peroxide) and O_{14} (carbonyl) are those that show the most negative values, an indication that negative charge density on artemisinin concentrates on the peroxide group and on the carbonyl group. When compared to the values obtained with the 6-31G(d) basis it may be seen that the bigger basis set tends to attribute higher negative charge density on O_{11}, O_{13}, and O_{14}, with both methods, and lower negative density on the peroxide group. The same behavior is followed by the intermediate basis set (hybrid basis set 2). Although these results may indicate a possible interaction of artemisinin with an electron poor group by means of the carbonyl group, this would have little effect on the peroxide group, well-known as the most relevant group in artemisinin for its antimalarial activity. In addition, these results also show that charge densities are strongly dependent on basis set and are given here only as reference to make a comparison. When analyzing the two oxygen atoms of the peroxide group the 6-31G(d) basis set and the hybrid basis set 2 show higher Mulliken charge density on O_1 than on O_2, while the hybrid basis set 1 shows the opposite. On the other hand, MK charge densities are higher on O_2 than on O_1.

Table 1. B3LYP atomic charge density (Mulliken and Merz–Kollman) for selected atoms of artemisinin using the hybrid basis set 1 (STO-3G + 3-21G), hybrid basis set 2 (3-21G + 6-31G(d)) and the 6-31G(d) basis set

Atom	Atomic charges (e^-)					
	STO-3G + 3-21G		3-21G + 6-31G(d)		6-31G(d)	
	Mulliken	MK	Mulliken	MK	Mulliken	MK
O_1	−0.279	−0.275	−0.307	−0.212	−0.326	−0.210
O_2	−0.320	−0.321	−0.276	−0.283	−0.294	−0.280
O_{11}	−0.129	−0.321	−0.522	−0.535	−0.476	−0.472
O_{13}	−0.176	−0.336	−0.468	−0.544	−0.516	−0.506
O_{14}	−0.380	−0.555	−0.660	−0.482	−0.454	−0.477

3.1.2. Geometric parameters. Artemisinin geometric parameters obtained with the 6-31G(d) basis set were compared to those obtained with the hybrid basis sets 1 and 2 (Table 2 and Fig. 1) as well as to values from X-ray experimental measurements.[24,25] For the relevant O_1–O_2 distance the difference between the 6-31G(d) result and the experimental data is 0.009–0.014 Å. In contrast, the differences found with the hybrid basis sets 1 and 2 are considerably larger, 0.046–0.051 Å and 0.012–0.017 Å, respectively. Similar behavior was observed for two selected distances, C_{12a}–O_1 and C_3–O_2. Notwithstanding, the values calculated with the hybrid basis set 2 are closer to those calculated with the 6-31G(d) basis set. A consequence of this fact is that C_{12a}–O_1 and C_3–O_2 distances calculated with the hybrid basis set 2 are closer to the experimental data than the corresponding 6-31G(d) values. Analysis of charge and geometric parameters indicates that the hybrid basis set 2 shows values that are close enough to the 6-31G(d) basis set and to experimental measurements.

3.2. DFT calculations for the heme group

The heme group has a Fe^{2+} ion coordinated to four pirrolic nitrogen atoms making the porphyrin ring.[29,30]

Table 2. Selected geometric parameters for artemisinin using the hybrid basis set 1 (STO-3G and 3-21G), hybrid basis set 2 (3-21G and 6-31G(d)), and the 6-31G(d) basis set. Some data from reference works are also indicated

Structure	Geometric parameter (Å)		
	C_{12a}–O_1	C_3–O_2	O_1–O_2
Hybrid basis set 1	1.527	1.489	1.520
Hybrid basis set 2	1.464	1.415	1.457
6-31G(d)	1.455	1.414	1.460
HF/6-31G(d)[26]	1.429	1.396	1.390
HF/6-31G(d)[27]	—	1.396	1.390
HF/6-31G[28]	1.469	1.435	1.447
Experimental[24]	1.461	1.416	1.469
Experimental[25]	1.450	1.418	1.474

Within hemoglobin, the Fe^{2+} ion is additionally coordinated to a histidine residue in an axial position (Fig. 2). The histidine residue was included in our calculations in order to have a model as close as possible to the real system. The minimum energy structure of heme has a conformation where the pairs of α and β carbons forming the border of the pirrolic rings are located up and down of the medium plane of porphyrin, respectively, while the meso carbon atoms are in the plane[31] (Fig. 2).

3.2.1. Relative energies for the several electronic states of heme. The DFT calculations show that the most stable electronic state of heme is the quintet state (Table 3), in agreement with previous high level calculations for porphine.[32] This state originates from a $3d^6$ electronic configuration on the Fe^{2+} ion, with the highest possible number of unpaired electrons. This result indicates that the ligand field around the Fe^{2+} ion is weak, resulting in a high spin complex. The triplet state is only mildly less stable, whereas the singlet state is significantly less stable. The septet state, on the other hand, is much less stable, which is understandable if we analyze the Fe^{2+} electronic configuration. The septet state may be obtained only by the promotion of one of the $3d^6$ electrons to a higher energy level. It was calculated only to help comparison when the complex with artemisinin is formed. The energy difference between the triplet and the quintet states is less than 2.0 kcal/mol in the different basis sets.

Table 3. B3LYP relative energies of heme using the hybrid basis set 1 (STO-3G + 3-21G), the hybrid basis set 2 (3-21G + 6-31G(d)), and the 6-31G(d) basis set

Structure	Relative energies (kcal/mol)		
	STO-3G + 3-21G	3-21G + 6-31G(d)	6-31G(d)
Singlet	4.91	4.44	5.44
Triplet	2.04	1.49	0.95
Quintet	0.00	0.00	0.00
Septet	38.94	36.84	25.22

3.2.2. Heme geometric parameters. The most relevant geometric parameter in heme is the coordination distance iron–nitrogen. Except for the singlet state, the distances between the Fe^{2+} ion and the pirrolic nitrogens are lower than the distances between Fe^{2+} and the imidazolic nitrogen of the histidine residue (Table 4 and Fig. 3). The differences are, however, dependent on the spin state. For instance, for the hybrid basis set 1, the difference reduces from the triplet spin state to the quintet spin state, and increases from the quintet spin state to the septet spin state. The septet spin state has a more distorted geometric arrangement than the triplet and the quintet spin states, as shown by the values of the dihedral angle C_α–C_m–C_α–N (Table 4). This dihedral angle is usually taken as a measure of the degree of non-planarity of the porphirinic ring.[33] The hybrid basis set 2 exhibits similar behavior, however, with the quintet spin state more distorted than the other electronic states. The 6-31G(d) basis set reproduces the results of the hybrid basis set 1 regarding the degree of planarity. However, in relation to the Fe–N distances, the 6-31G(d) basis set results are closer to those obtained with the hybrid basis set 2. The angle N–Fe–N tends to decrease with increasing multiplicity. This can be seen when one compares the theoretical calculations of different spin states.

3.2.3. Atomic charges and spin densities. Charge densities on the pirrolic nitrogen atoms are negative and almost evenly distributed, as shown in Table 5. In contrast, the iron atom has positive charge density. The results obtained with the hybrid basis set 1 show that the atomic charge values for triplet, quintet, and septet electronic states are very similar, although there is a small increase in the positive charge on the Fe^{2+} ion, with a corresponding increase in the negative charge on the nitrogens coordinated to it, when increasing the multiplicity from singlet, to triplet, quintet, and septet. The same behavior is calculated with both the hybrid basis set 2 and the 6-31G(d) basis set. Regarding spin density, for the triplet and quintet states, the spin densities are completely concentrated on the iron atom (Table 5), while in

Table 4. UB3LYP geometric parameters obtained with the hybrid basis set 1 (STO-3G + 3-21G), the hybrid basis set 2 (3-21G + 6-31G(d)), and the 6-31G(d) basis set for heme group coordinated to a histidine residue

Structure		Geometric parameter (Å)					
		$Fe–N_4$	$Fe–N_8$	$Fe–N_{76}$	$N_4–Fe–N_{17}$	$N_8–Fe–N_{25}$	$C_\alpha–C_m–C_\alpha–N$
Singlet	Hybrid basis set 1	2.022	2.018	1.943	171.1	170.0	1.97
	Hybrid basis set 2	2.011	2.006	1.938	179.2	175.4	1.96
	Single basis set	2.000	1.992	1.931	177.6	170.3	1.88
Triplet	Hybrid basis set 1	2.037	2.032	2.219	172.4	168.5	1.99
	Hybrid basis set 2	2.011	2.023	2.295	173.6	172.1	1.54
	Single basis set	1.993	2.017	2.249	173.1	170.8	1.78
Quintet	Hybrid basis set 1	2.091	2.109	2.154	160.8	164.5	1.57
	Hybrid basis set 2	2.087	2.099	2.197	162.1	166.1	2.47
	Single basis set	1.988	1.994	2.182	177.7	171.4	1.58
Septet	Hybrid basis set 1	2.092	2.096	2.133	159.6	163.7	2.86
	Hybrid basis set 2	2.075	2.069	2.124	158.5	163.9	2.15
	Single basis set	2.064	2.064	2.105	158.5	163.8	1.93
Experimental[34]		2.061	2.052	2.233	152.1	152.1	0.04

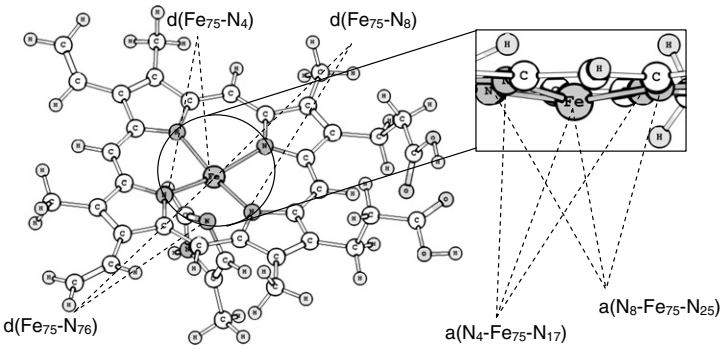

Figure 3. Definition of geometric parameters for the heme group coordinated to a histidine residue.

Table 5. UB3LYP atomic charges and spin densities on selected atoms of the heme group calculated with the hybrid basis set 1 (STO-3G + 3-21G), the hybrid basis set 2 (3-21G + 6-31G(d)), and the 6-31G(d) basis set

Structure			Atom					
			N_4	N_8	N_{17}	N_{25}	Fe_{75}	N_{76}
Singlet	Hybrid basis set 1	Charge	−0.307	−0.309	−0.312	−0.309	0.696	−0.211
	Hybrid basis set 2	Charge	−0.671	−0.683	−0.664	−0.701	0.795	−0.555
	Single basis set	Charge	−0.773	−0.786	−0.767	−0.795	1.196	−0.486
Triplet	Hybrid basis set 1	Charge	−0.291	−0.326	−0.308	−0.329	0.655	−0.184
		Spin	−0.013	−0.017	−0.019	−0.016	2.011	0.046
	Hybrid basis set 2	Charge	−0.701	−0.723	−0.678	−0.729	0.821	−0.541
		Spin	−0.021	−0.022	−0.014	−0.021	2.025	0.041
	Single basis set	Charge	−0.790	−0.804	−0.775	−0.805	1.182	−0.494
		Spin	−0.030	−0.030	−0.021	−0.031	2.128	0.041
Quintet	Hybrid basis set 1	Charge	−0.339	−0.320	−0.343	−0.323	0.739	−0.168
		Spin	0.055	0.058	0.056	0.058	3.709	0.038
	Hybrid basis set 2	Charge	−0.767	−0.735	−0.761	−0.742	1.035	−0.585
		Spin	0.055	0.059	0.055	0.058	3.725	0.038
	Single basis set	Charge	−0.836	−0.824	−0.831	−0.834	1.353	−0.523
		Spin	0.044	−0.054	0.048	−0.051	2.886	0.083
Septet	Hybrid basis set 1	Charge	−0.353	−0.331	−0.357	−0.369	0.837	−0.232
		Spin	0.237	0.186	0.273	0.075	3.862	0.059
	Hybrid basis set 2	Charge	−0.786	−0.769	−0.782	−0.776	1.263	−0.640
		Spin	0.256	0.149	0.275	0.138	4.002	0.090
	Single basis set	Charge	−0.866	−0.858	−0.864	−0.859	1.470	−0.576
		Spin	0.192	0.084	0.201	0.090	4.242	0.069

Atomic charges are given in e^-.

the septet state some spin density is also found on the nitrogen atoms. As was observed for artemisinin the results obtained with the 6-31G(d) basis set are closer to those obtained with the hybrid basis set 2 than to the results obtained with the hybrid basis set 1.

3.3. DFT calculations for complexes between heme and artemisinin

Previous calculations for the interaction between artemisinin and the heme group had been done using molecular mechanics[35,36] and semi-empirical methods such as MNDO/d,[37] PM3(tm),[38] and PM3.[39,40] Due to the advance in computational processing power in the last few years, more refined techniques have become available, and DFT methods have been established as one of the main methods for calculations on organic molecules.[41] Although the 6-31G(d) basis set has become standard,[42] it is still necessary to evaluate the ability of smaller combinations of basis set to reproduce properties of large systems, such as those studied in the present work.

The three electronic spin states triplet, quintet, and septet were calculated for the artemisinin–heme complex. As shown above, the thermodynamically most stable spin state for the isolated heme group is the quintet state. So, it could be predicted that for artemisinin–heme interactions at long distances this should also be the most stable state. However, for interactions at short distances, both the triplet and the septet states may become more stable.

3.3.1. Heme–artemisinin interaction energies. Calculations were performed on several points along the potential energy surface approaching artemisinin and the heme group in the three spin states. Therefore, we could construct three energy curves relating energy to the dis-

tance between the iron atom of heme and the oxygen O_2 of the peroxide group (Fig. 4). With the hybrid basis set 1 when interacting at short distances, the triplet spin state is less stable (Fig. 4 and Table 6). Because of this, and considering that at long distances the system would behave as isolated artemisinin and heme, the triplet spin state was calculated only with the smaller basis set. Results for the quintet and septet states using the hybrid basis set 2 indicate that at a distance of 3.0 Å the quintet spin state is more stable than the septet state by 35.2 kcal/mol (Figs. 4 and 5, Table 6). These results agree with molecular mechanics studies for the interaction between heme and artemisinin which show that in the most stable complex the distance between O_2 oxygen atom of artemisinin and the Fe^{2+} ion is about 2.65 Å and the complex is more stable at long distances.[35] Molecular mechanics calculations using docking methodology indicate that the interaction energy at long distances has values of −30 to −33 kcal/mol.[36] In the present work, for interaction at long distances, we calculated an interaction energy of −5.6 kcal/mol.

Analysis of the potential energy curves for the quintet and the septet spin states show that during the formation of the heme–artemisinin covalent bond, the decrease of energy for the septet spin state is more intense than for the quintet spin state, as seen in Figure 4. Thus, although the energy difference between the two states is considerably high at long distances, as the two

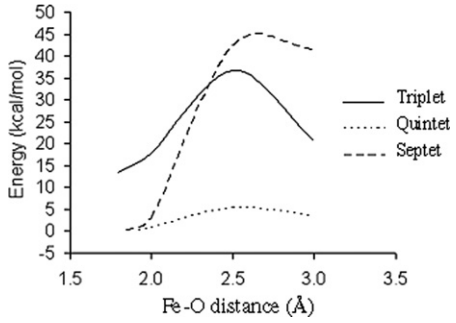

Figure 4. Relative energies (kcal/mol) as a function of the distance between the Fe^{2+} ion of the heme group and the oxygen atom O_2 of artemisinin.

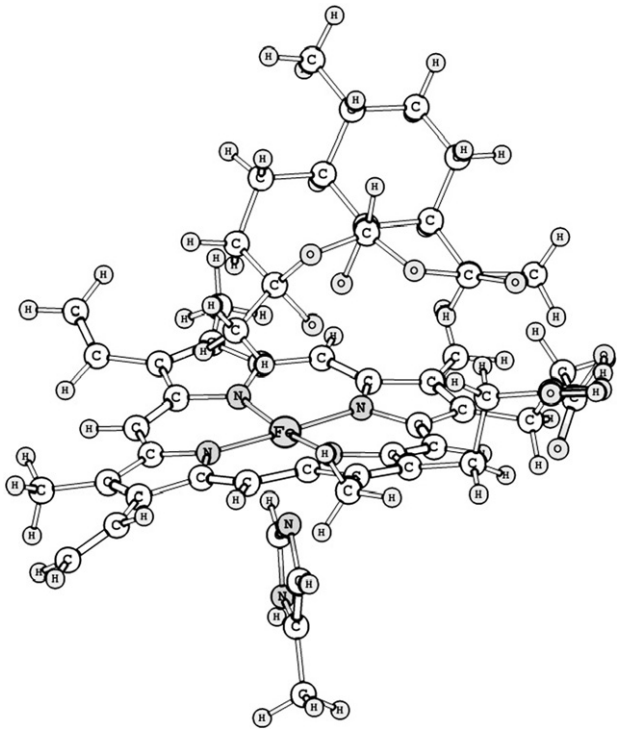

Figure 5. Most stable complex between heme and artemisinin at a long distance (quintet spin state).

unities approach each other the energy difference decreases and becomes almost isoenergetic at short distances. In the final full optimized geometry of the adduct, the septet spin state is only 1.4 kcal/mol more stable than the quintet spin state (Fig. 4 and Table 6). These results accord to expectation if we consider that upon oxidation of the heme group and reduction of artemisinin, two new unpaired electrons are yielded. Therefore, the septet spin state should result from a d^5 electronic configuration on the Fe^{3+} ion of the heme group summed up with an unpaired electron on the O_1 oxygen atom of artemisinin (see Fig. 6).

3.3.2. Electron transfer. An important point in the potential energy surface for interaction between artemisinin and heme is the electron transfer step that occurs when heme reduces artemisinin. The electron transfer reaction may be represented by the general equation:

Table 6. UB3LYP relative and interaction energies for heme–artemisinin complexes calculated with the hybrid basis set 1 (STO-3G + 3-21G) and the hybrid basis set 2 (3-21G + 6-31G(d))

Fe–O_2 distance	Relative energy (kcal mol^{-1})			Interaction energy[a] (kcal mol^{-1})		
	Triplet[b]	Quintet	Septet	Triplet[b]	Quintet	Septet
Adduct[c]	13.30	1.44	0.00	−3.19	0.01	−1.45
2.0	17.75	2.38	3.08	1.25	0.92	1.62
2.25		0.99	11.45		−0.46	9.65
2.5	36.61	−1.98	18.06	20.12	−3.43	16.60
2.75		−5.25	34.96		−6.71	33.50
3.0	20.71	−4.07	31.17	4.22	−5.53	29.71

[a] The interaction energy was calculated using the energy of the optimized ground quintet state of heme and the energy of optimized singlet artemisinin.

[b] The values for the triplet state were obtained with the hybrid basis set 1.

[c] The O_2–Fe bond distances for the heme–artemisinin adduct in the triplet, quintet, and septet spin states are 1.801 Å, 1.919 Å and 1.848 Å, respectively.

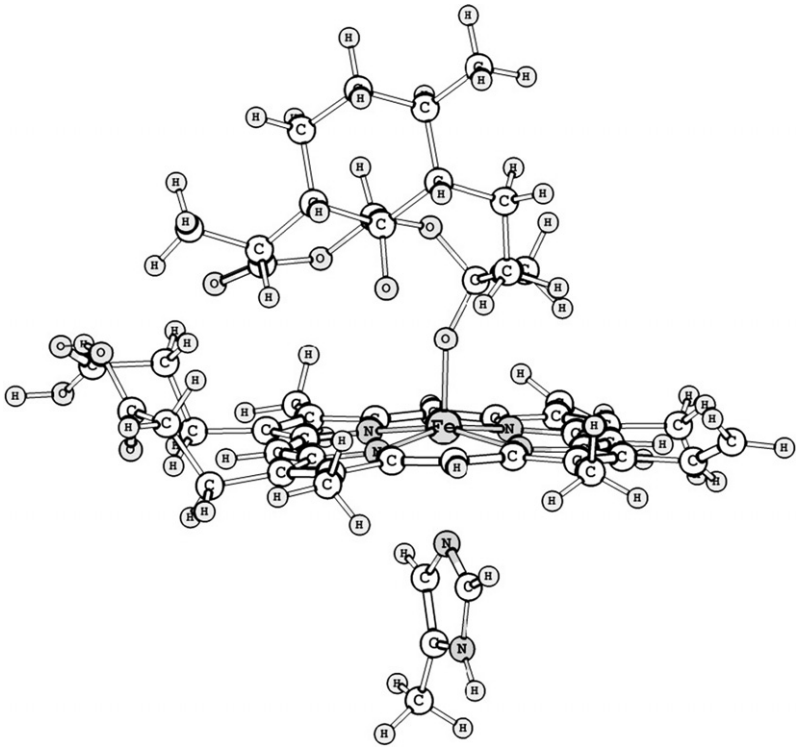

Figure 6. Optimized geometry for the most stable heme–artemisinin adduct at short O_2–Fe_{75} distance (septet spin state).

$$\text{Heme(Fe(II))} + \text{artemisinin} \rightarrow \text{Heme(Fe(III))} + \text{artemisinin}^{-}$$

Although the calculation of such electron transfer may not follow usual procedures, we can at least give an approximation to the energy involved in the electron transfer. The point on the potential energy surface where electron transfer may take place is that where the curves for the two involved electronic states cross. Localization of this point on a potential energy surface using traditional methodology is not a simple task due to the many degrees of freedom involved. An approximation to it, however, is possible by calculating the two curves separately and identifying the approximate geometry where the curves cross. This would give a range between two points on the potential energy curve where the electron transfer may take place. Following this methodology we built two graphics, one for the quintet spin state and another for the septet spin state. Each of these graphics shows two curves of relative energy versus distance between the iron atom and the oxygen atom O_2 (Figs. 7 and 8). One curve is for the electronic configuration of the reactants, where the peroxide bond has not yet been broken. The other curve is for the electronic configuration of the products, with the peroxide bond broken. The intersection of these curves gives a limit to the activation energy for the electron transfer process.[43]

For the quintet state in the reactant electronic configuration, with intact peroxide bond (curve 2, Fig. 7), the minimum energy is found for a distance of about 2.75 Å. As the heme group and artemisinin approach each other at a distance lower than 2.5 Å the energy considerably increases. When considering the product electronic configuration, the minimum energy point is found for a distance of 1.92 Å. As the heme–artemisinin distance increases the relative energy also considerably increases. The intersection with the reactant curve is found at a distance between 2 and 2.25 Å. This is the point along the quintet potential energy surface where electron transfer may take place, with activation energy in the order of 10 kcal/mol, as indicated in Figure 7.

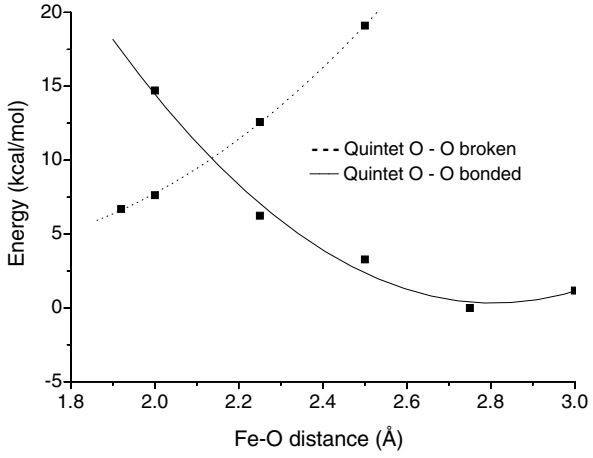

Figure 7. Relative energy as a function of the distance between the iron atom of heme and the oxygen atom O_2 of the artemisinin peroxide group for the quintet spin state.

Similar curves can be constructed for the septet spin state (Fig. 8). As shown, however, in this case the curve for the reactant electronic configuration has much higher energy

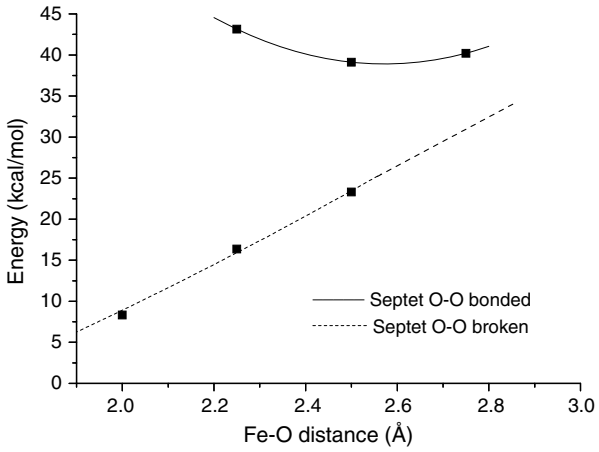

Figure 8. Relative energy as a function of the distance between the iron atom of heme and the oxygen atom O_2 of artemisinin for the septet spin state.

than the curve for the product electronic configuration. The two curves seem to approach each other only at very long distances between the two unities. For distances below 3 Å in the septet spin state the configuration with the broken peroxide bond is always much more stable than the corresponding curve in the reactant electronic configuration. It means that in the septet spin state the complex exists only with the broken peroxide bond. In this electronic state, artemisinin adds to the heme group without activation energy. On the other hand, if we consider that electron transfer occurs between 2.0 and 2.25 Å, according to the results for the quintet spin state, this would yield the septet potential energy surface where energy goes down for distances below 2.25 Å. These results led us to conclude that at long artemisinin–heme distances the system exists in the quintet spin state, forming an initial complex with interaction energy of 5.6 kcal/mol. This initial complex may thus evolve to the adduct, after one electron is transferred from the heme group to artemisinin. This electron transfer would occur when the heme–artemisinin distance is between 2.0 and 2.25 Å, and should involve activation energy in the order of 10 kcal/mol. The electron transfer yields the septet spin state which is the most stable state for the heme–artemisinin adduct (see Table 6 for relative energies and Table 7 for selected geometrical parameters of the most stable heme-artemisinin complexes).

Previous calculations for model systems[44] reported the triplet state as the most stable, reproducing relative stabilities calculated for porphyrin at the same computational level. However, high level computations for iron(II) porphine clearly indicate the quintet as the lowest state,[32] in agreement with results given in the present work. It was also suggested that there should be a small energy barrier to opening the endoperoxide bond of artemisinin,[44] a result that is confirmed in the present study.

Table 7. UB3LYP geometric parameters calculated using the hybrid basis set 1 (STO-3 G + 3-21G) and the hybrid basis set 2 (3-21G + 6-31G(d)) for the most stable heme–artemisinin complexes

Structure		Geometric parameters (Å)		
		O_1–O_2	O_2–Fe_{75}	N_{76}–Fe_{75}
Quintet	Hybrid basis set 1	1.520	3.021	2.187
		2.391	1.919	2.411
	Hybrid basis set 2	2.995	1.889	2.436
Septet	Hybrid basis set 1	2.562	1.848	2.392
	Hybrid basis set 2	3.009	1.842	2.430

4. Conclusions

The DFT calculations for artemisinin reveal that the hybrid basis set 2 and the 6-31G(d) basis set attribute higher charge density on O_{11}, O_{13}, and O_{14} and lower charge density on the peroxide group. Although this might indicate a preferential interaction of artemisinin by means of the carbonyl group, this interaction should have no effect on the peroxide group. Regarding the relevant geometric parameters, the results show that the hybrid basis set 1 has a strong tendency to yield bond distances that are greater than the experimental values. On the other hand, the hybrid basis set 2 and the 6-31G(d) basis set agree with each other and give values that are closer to the experimental data. For heme, the DFT calculations with the hybrid and the 6-31G(d) basis sets show that the quintet spin state is more stable than the triplet, singlet, and septet spin states, in this order. The 6-31G(d) results show the septet spin state as the most distorted. Positive charges as well as spin density are found on the iron atom of heme.

For the complexes between heme and artemisinin the quintet spin state is the most stable at long distances, being 17.4 kcal/mol and 39.1 kcal/mol, respectively, more stable than the triplet and the septet spin states. At short distances the septet spin state is 1.4 kcal/mol more stable than the quintet spin state.

Although the exact geometry for electron transfer could not be determined, approximate evaluation of the electron transfer process was possible. This indicated that at long distances the heme–artemisinin complex exists in the quintet state. As both moieties approach each other, in distances of 2.0–2.25 between the Fe atom of heme and the O_2 oxygen of artemisinin, electron transfer from the heme group to artemsinin may occur, with activation energy about 10 kcal/mol. At short distances, in the geometry of the adduct, the heme–artemisinin complex exists in the septet spin state, with the quintet spin state only slightly higher in energy. Thus, we could find that artemisinin may interact with the heme group with negative stabilization energy and that electron transfer from heme to artemisinin involves low activation energy, supporting the suggestion that artemisinin reduction may be an important step for its activation.

Acknowledgments

We acknowledge financial support from CAPES, CNPq (Proc. No. 478954/2001-8), UEFS, and FAPESB (PPP-7731-2006). F.H.A. Leite is also grateful to FAPESB for his fellowship.

Supplementary data

Supplementary data associated with this article can be found, in the online version, at doi:10.1016/j.bmc.2008.03.033.

References and notes

1. Neves, P. D. *Parasitologia Humana*; Rio de Janeiro: Livraria Atheneu, 1998.
2. Dhingra, K. V. *Biochem. Education* **1999**, *27*, 105.
3. OMS, http://www.who.int/mediacentre/factsheets/fs094/en/. Accessed on February 2005.
4. Robert, A.; Meunier, B. *Chem. Soc. Rev.* **1998**, *27*, 273.
5. Balint, G. A. *Pharmacol. Ther.* **2001**, *90*, 261.
6. Haynes, R. K. *Curr. Opin. Infect. Dis.* **2001**, *14*, 719.
7. Meshnick, S. R. *Int. J. Parasitol.* **2002**, *32*, 1655.
8. Meshnick, S. R.; Jefford, C. W.; Posner, G. H.; Avery, M. A.; Peters, W. *Parasitol. Today* **1996**, *12*, 79.
9. Pandey, A. V.; Tekwani, B. L.; Singh, R. L.; Chauhan, V. S. J. *J. Biol. Chem.* **1999**, *274*, 19383.
10. Jefford, C. H.; Favager, F.; Vicente, M. G. H.; Jacquier, Y. *Helv. Chim. Acta* **1995**, *78*, 452.
11. Haynes, R. K.; Vonwiller, S. C. *Tetrahedron Lett.* **1996**, *37*, 253.
12. Haynes, R. K.; Vonwiller, S. C. *Tetrahedron Lett.* **1996**, *37*, 257.
13. Wu, W. M.; Wu, Y.; Wu, Y. L.; Yao, Z. J.; Zhou, C. M.; Li, Y.; Shan, F. *J. Am. Chem. Soc.* **1998**, *120*, 3316.
14. Arantes, C.; Taranto, A. G.; Araújo, M. T.; Carneiro, J. W. M. *Int. J. Quantum Chem.* **2005**, *103*, 749.
15. Araújo, M. T.; Taranto, A. G.; Carneiro, J. W. M. *Int. J. Quantum Chem.* **2006**, *106*, 2804.
16. Taranto, A. G.; Carneiro, J. W. M.; Araújo, M. T. *Bioorg. Med. Chem.* **2006**, *14*, 1546.
17. Sibmooh, N.; Udomsangpetch, R.; Kijjoa, A.; Chantharaksri, U.; Mankhetkorn, S. *Chem. Pharm. Bull.* **2001**, *12*, 1541.
18. Becke, A. D. *J. Chem. Phys.* **1993**, *98*, 5648.
19. Lee, C. T.; Yang, W. T.; Parr, R. G. *Phys. Rev. B* **1988**, *37*, 785.
20. Vosko, S. H.; Wilk, L.; Nusair, M. *Can. J. Phys.* **1980**, *58*, 1200.
21. Dunning, T. H., Jr.; Hay, P. J. In *Modern Theoretical Chemistry v. 3*, Schaefer, H. F., III, Ed.; v. 3, New York, 1976.
22. Frisch, M. J.; Trucks, G. W.; Schlegel, H. B.; Scuseria, G. E.; Robb, M. A.; Cheeseman, J. R.; Montgomery, J. A., Jr.; Vreven, T.; Kudin, K. N.; Burant, J. C.; Millam, J. M.; Iyengar, S. S.; Tomasi, J.; Barone, V.; Mennucci, B.; Cossi, M.; Scalmani, G.; Rega, N.; Petersson, G. A.; Nakatsuji, H.; Hada, M.; Ehara, M.; Toyota, K.; Fukuda, R.; Hasegawa, J.; Ishida, M.; Nakajima, T.; Honda, Y.; Kitao, O.; Nakai, H.; Klene, M.; Li, X.; Knox, J. E.; Hratchian, H. P.; Cross, J. B.; Adamo, C.; Jaramillo, J.; Gomperts, R.; Stratmann, R. E.; Yazyev, O.; Austin, A. J.; Cammi, R.; Pomelli, C.; Ochterski, J. W.; Ayala, P. Y.; Morokuma, K.; Voth, G. A.; Salvador, P.; Dannenberg, J. J.; Zakrzewski, V. G.; Dapprich, S.; Daniels, A. D.; Strain, M. C.; Farkas, O.; Malick, D. K.; Rabuck, A. D.; Raghavachari, K.; Foresman, J. B.; Ortiz, J. V.; Cui, Q.; Baboul, A. G.; Clifford, S.; Cioslowski, J.; Stefanov, B. B.; Liu, G.; Liashenko, A.; Piskorz, P.; Komaromi, I.; Martin, R. L.; Fox, D. J.; Keith, T.; Al-Laham, M. A.; Peng, C. Y.; Nanayakkara, A.; Challacombe, M.; Gill, P. M. W.; Johnson, B.; Chen, W.; Wong, M. W.; Gonzalez, C.; Pople, J. A. *Gaussian 03, Revision A.1*; Gaussian, Inc.: Pittsburgh, PA, 2003.
23. Singh, U. C.; Kollman, P. *J. Comput. Chem.* **1984**, *5*, 129.
24. Lisgarten, J. N.; Potter, B. S.; Bantuzeko, C.; Palmer, R. A. *J. Chem. Crystallogr.* **1998**, *28*, 539.
25. Leban, I.; Golic, L.; Japelj, M. *Acta Pharm. Jugosl.* **1988**, *38*, 71.
26. Pinheiro, J. C.; Kiralj, R.; Ferreira, M. M. C. *QSAR Comb. Sci.* **2003**, *22*, 830.
27. Bernardinelli, G.; Jefford, C. W.; Maric, D.; Thomson, C.; Weber, J. *Int. J. Quant. Chem.* **1994**, *21*, 117.
28. Pinheiro, J. C.; Kiralj, R.; Ferreira, M. M. *J. Mol. Struct. (Theochem.)* **2001**, *572*, 35.
29. Cowan, J. A. *Inorganic Biochemistry: An Introduction*; VHC Publishers: New York, 1993.
30. Silva, J. J. R. F.; Williams, R. J. P. *The Inorganic Chemistry of Life*; Charendon Press: New York, 1993.
31. Munro, O. Q.; Bradley, J. C.; Hancock, R. D.; Marques, H. M.; Marsicano, F.; Wade, P. W. *J. Am. Chem. Soc.* **1992**, *144*, 7218.
32. Choe, Y.-K.; Nakajima, T.; Hirao, K.; Lindh, R. *J. Chem. Phys.* **1999**, *111*, 3837.
33. Zhang, Y. H. *Chem. Phys.* **2005**, *315*, 201.
34. Frier, J. A.; Perutz, M. *J. Mol. Biol.* **1977**, *112*, 97.
35. Shukla, K. L.; Gund, T. M.; Meshnick, S. R. *J. Mol. Graphics* **1995**, *13*, 215.
36. Tonmunphean, S.; Parasuk, V.; Kokpol, S. *J. Mol. Graphics* **2001**, *7*, 26.
37. Taranto, A. G.; Carneiro, J. W. M.; Oliveira, F. G. *J. Mol. Struct. (Theochem.)* **2001**, *539*, 267.
38. Taranto, A. G.; Carneiro, J. W. M.; Araújo, M. T.; Silva, B. G. *Sitientibus* **2006**, *34*, 47.
39. Taranto, A. G.; Carneiro, J. W. M.; Oliveira, F. G.; Araújo, M. T.; Correa, C. R. *J. Mol. Struct. (Theochem.)* **2002**, *580*, 207.
40. Costa, M. S.; Kiralj, R.; Ferreira, M. M. C. *Quim. Nova* **2007**, *30*, 25.
41. Morgon, N. H.; Custódio, R. *Quim. Nova* **1995**, *18*, 44.
42. Young, D. *Computational Chemistry: A Practical Guide for Applying Techniques to Real World Problems*; John Wiley & Sons: New York, 2001.
43. Marcus, R. A. *Annu. Rev. Phys. Chem.* **1964**, *15*, 155.
44. Drew, M. G. B.; Metcalfe, J.; Ismail, F. M. D. *J. Mol. Struct. (Theochem.)* **2004**, *711*, 95.